Metrol. Meas. Syst., Vol. XX (2013), No. 2, pp. 307–322.

PAN POLSKA AKADEMIA NAUK

METROLOGY AND MEASUREMENT SYSTEMS

Index 330930, ISSN 0860-8229

www.metrology.pg.gda.pl

M&MS

KALMAN FILTER BASED METHOD FOR FAULT DIAGNOSIS OF ANALOG CIRCUITS

Xifeng Li, Yongle Xie, Dongjie Bi, Yongcai Ao

School of Automation Engineering, University of Electronic Science and Technology of China, Chengdu, 611731, China
(✉ yonglexie@hotmail.com. +86-13708083375, xfengl@hotmail.com, bidongjie1985@126.com, darrenao@hotmail.com)

Abstract

This paper presents a Kalman filter based method for diagnosing both parametric and catastrophic faults in analog circuits. Two major innovations are presented, i.e., the Kalman filter based technique, which can significantly improve the efficiency of diagnosing a fault through an iterative structure, and the Shannon entropy to mitigate the influence of component tolerance. Both these concepts help to achieve higher performance and lower testing cost while maintaining the circuit's functionality. Our simulations demonstrate that using the Kalman filter based technique leads to good results of fault detection and fault location of analog circuits. Meanwhile, the parasitics, as a result of enhancing accessibility by adding test points, are reduced to minimum, that is, the data used for diagnosis is directly obtained from the system primary output pins in our method. The simulations also show that decision boundaries among faulty circuits have small variations over a wide range of noise-immunity requirements. In addition, experimental results show that the proposed method is superior to the test method based on the subband decomposition combined with coherence function, arisen recently.

Keywords: Analog fault diagnosis, signature extraction, Kalman filter, Shannon entropy.

1. Introduction

Testability of analog circuits has become more important recently due to the rapid development in analog VLSI chips, mixed-signal systems, and system-on-chip (SoC) products [1]-[3]. Since complete testing of an analog circuit specification can be costly, sometimes impossible, analyzing the output response of the circuit under test (CUT), which is called signature analysis, is the key to successful application of defected-oriented testing for high fault and yield coverage [4].

Signature analysis in analog circuits is complicated because the uncertainty comes from the poor input signal and tolerances in the component values of the analog circuit [4]. Further, the imprecise measurement of the analog circuit can also cause the response of the circuit to be different from the ideal response. These make it mandatory to compress the output response in order to produce a signature of the output for fault diagnosis.

Unfortunately, the signature of the faulty response may correspond to a fault-free signature, which is usually called aliasing. The aliasing results in a failure of fault diagnosis. Further, aliasing may also happen if the signature of the faulty response is not robust. Our motivation for this research is to minimize the aliasing probability by incorporating noise information in generating the robust signature.

2. Preliminaries and Contributions

A significant amount of methods dealing with signature analysis in analog circuits has been proposed, and only some of them are reviewed here. First, several important schemes are

Article history: received on Jan. 11, 2013; accepted on May. 20, 2013; available online on Jun. 03, 2013; DOI: 10.2478/mms-2013-0027.

briefly reviewed, and then the noise-based signature extraction scheme, on which our technique is based, is discussed.

2.1. Previous work

Papakostas and Hatzopoulos [5] proposed a correlation-based comparison of the analog signatures scheme for improving the fault discrimination capacity, which introduced a new criterion by the use of a weighted factor. Faults in the CUT that lead to similar analog signatures can be detected and identified. This approach is appealing since the probability of aliasing is sharply reduced. Subband filtering testing using an integrator scheme for analog response signature compacting was proposed in [4]. In this scheme, a subband filter takes the test response, and then decomposes the signal for each frequency band. The decomposed signal for each frequency band is then fed into its respective integrator, which was used for signature compression. This scheme has good performance on parameter faults and catastrophic faults.

Catelani and Fort [6] proposed an efficient scheme for analyzing signatures of analog circuits using a radial basis function network classifier. Their main idea is to use neural networks to perform fault diagnosis of analog circuits. The network is trained by means of a fault dictionary, which was previously constructed and contained examples of fault signatures. An index of the novelty of the fault is obtained as an output of the network, and this is used as an output of signature compression. It is assumed that the neural networks already exist as a part of the test overhead for the fault diagnosis.

Coefficient-based testing employing the bounds of circuit transfer-function coefficients as the signature is proposed by Guo and Savir [7], [8]. In their scheme, the values of the transfer-function coefficients of the good circuit are supposed to lie in their individual hypercubes. Whenever one or more of the CUT's coefficient values slip outside their hypercube, a different transfer function that reflects the existence of a detectable fault is obtained. Since this scheme tries to get the corresponding transfer-function, significant computational overhead is needed.

In [9], Yang et al. combined the slope-based model and the test-point selection algorithm for analog circuits test. In this scheme, the slope is used for signature compression. Although the slope signature can diagnose both parametric and catastrophic faults, it leads to a significant computational cost. Deng et al. [10] propose a new approach based on the subband decomposition combined with coherence functions. Their main idea is that the Volterra kernel is decomposed in subband, and the decomposed response signals are processed by a coherence function to extract the fault signature. Since this scheme requires computing the Volterra series and coherence function, the significant computational cost is also considerable.

2.2. Work in this paper

From above illustrations of the previous work, it is easily seen that traditional methods for fault diagnosis of analog circuits are mainly focused on the fault location at the cost of augmenting the algorithm complexity or adding the test nodes for data acquisition. A robust method, which could explore the information contained in the measurement data of the CUT as much as possible without adding additional test nodes, is appealing. Meanwhile, the method should identify the new information from the new measured data without acquiring more complexity of the algorithm, with aid of this information, a robust and sensitive signature can be obtained so effectively that the fault location becomes more reliable and robust.

Thanks to the Kalman filter technique, the objective that we want to fulfil the above task can be easily achieved. To the best knowledge of the authors, the Kalman filter based method for fault diagnosis of analog circuits has not been reported. Especially, the noise-based diagnosis method presented here is also new.

In this paper, the Kalman filter is used to acquire the variance of the Gaussian distribution, which is unique for a concrete fault. Based on the Gaussian distribution, the Shannon entropy is used as the signature parameter to identify the fault.

This paper focuses on locating the fault and minimizing the aliasing probability effectively when a parametric or catastrophic fault occurred in the analog circuit. Simulation and experimental results show the robustness of the proposed approach compared with the subband decomposition and coherence function based method [10]. The remainder of this paper is organized as follows: In section III, a fault model is established, the Kalman filter is reviewed, the Kalman filter based method for fault diagnosis of analog circuits is illustrated. Two simulations described in Section IV demonstrate the approach. Section V provides an experiment validation of the usefulness of the proposed method for fault diagnosis in an actual analog circuit. Conclusions are given in Section VI.

3. Diagnosis method

3.1. Diagnosis model

In order to find the relation between fault-free and faulty output signals, a new fault model is proposed at first.

Due to the inherent uncertainty coming from the measurement and system disturbance, the output of the analog circuit may vary within an acceptable range around its nominal value and this will not be treated as a fault. Therefore, it is reasonable to assume that the ideal fault-free output is constant, i.e., ideal fault-free output is used as the nominal value. The actual fault-free response deviates from the ideal fault-free output peacefully. Otherwise, the circuit is supposed to be faulty.

So, the measured output of the analog circuit can be considered as the realization of a random process, in which the ideal fault-free output can be viewed as its mean value or nominal value.

With this in mind, the analog circuit testing can be viewed to address the problem of trying to extract the signature of the output signal $x \in R^n$ of the CUT that is governed by the linear stochastic difference equation

$$x_k = x_{k-1} + w_{k-1} \tag{1}$$

With a measurement $y \in R^n$ that is

$$y_k = x_k + v_k \tag{2}$$

The random variable w_{k-1} and v_k represent the process and measurement noise, respectively. They are assumed to be a normal probability distribution: $w_{k-1} \sim N(0, Q), v_k \sim N(0, R)$, where Q and R represent the process noise variance and measurement noise variance, respectively. The subscript k in (1) and (2) denotes the discrete time.

Remark 1: For analog circuits with a catastrophic fault, we are assuming that the measurement uncertainty v_k is fixed, that is, the variance of v_k stays constant during the process of measurement. x_k in (1), having a large deviation from the fault-free output, corresponds to w_{k-1} with a large variance.

Remark 2: For a parametric fault, if it is supposed that the measurement uncertainty v_k in (2) is fixed as explained in Remark 1, x_k in (1) shows a small deviation from the fault-free output, which corresponds to w_{k-1} with a small variance.

Remark3: There is no such thing as a perfect measurement. Measurement of the variable are influenced by a number of elemental error sources, such as errors caused by variations in ambient temperature, humidity, pressure, vibrations, electromagnetic influences; unsteadiness in the "steady-state" phenomenon being measured, and others. So, here, the measurement uncertainty is quantitatively described by v_k, which indicates the uncertainty introduced by the imperfect measurement.

3.2. Noise-enhanced testing scheme

The method of using suitable noise to enhance performance has been proposed as a powerful signal processing scheme [15], [16], [17]. However, to the best of the authors' knowledge, noise-aided fault diagnosis of analog circuits is rarely reported. A detailed discussion of the noise-enhanced fault diagnosis scheme will be given in this section, and the scheme proposed below is based on Kalman filtering.

In our scheme, recalling (1), the fault-free response and the white noise with a certain mean and variance make the output of the faulty circuit. Furthermore, because of the unique role of each component in analog circuits, it is reasonable to assume that the white noise corresponds one-to-one with a concrete component fault in the circuits. So, it is natural to use the white noise as the objective of the fault signature analysis.

The proposed scheme has a Kalman filter as the preprocessing block shown in Fig.1. The preprocessing block can be represented as the general Kalman filter with its filter characteristics depending on the application and specification of the CUT. The Kalman filter takes the response measured by the test equipment, then generates the result of noise estimation for the current state of the CUT. The noise is then fed into the signature generation blocks. The signature has its own fault-free value and unique error tolerance. At last, the classifier is used as a comparator to detect and locate faults in the CUT.

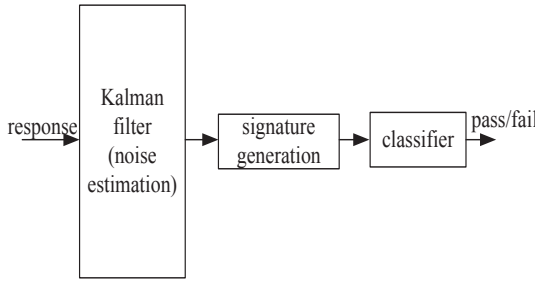

Fig. 1. Signature analysis scheme using Kalman filtering.

3.3. Kalman filtering

Since the Kalman filter is used as the main part of our proposed response compression scheme, an outlined discussion of the Kalman filter will be given in this section.

In 1960, R. E. Kalman published his famous paper describing a recursive solution to the discrete-data linear filtering problem [11]. Since that time, due in large part to advances in digital computation, the Kalman filter has been the subject of extensive research and application, particularly in the area of autonomous or assisted navigation. Theoretically, the Kalman filter is an estimator for what is called the linear-quadratic problem, which is the problem of estimating the instantaneous "state" of a linear dynamic system perturbed by white noise by using measurements linearly related to the state but corrupted by white noise. The resulting estimator is statistically optimal with respect to any quadratic function of estimation error. Practically, the Kalman filter provides a means for inferring the missing information from indirect and noisy measurement and is also used for predicting the likely future courses of dynamic systems that people are not likely to control [12].

The Kalman filter addresses the general problem of trying to estimate the state $x \in R^n$ of a discrete-time controlled process that is governed by the linear stochastic difference equation

$$x_k = Ax_{k-1} + Bu_{k-1} + w_{k-1} \tag{3}$$

with a measurement $z \in R^m$ that is

$$z_k = Hx_k + v_k \tag{4}$$

The random variables w_{k-1} and v_k represent the process and measurement noise, respectively. They are assumed to be independent of each other, white, and with normal probability distributions:

$$w_{k-1} \sim N(0, Q) \tag{5}$$

$$v_k \sim N(0, R) \tag{6}$$

where Q and R represent process noise covariance and measurement noise covariance, respectively.

In practice, the process noise covariance Q and measurement noise covariance R matrices might slightly change with each time step or measurement, however here we assume they are constant. The $n \times n$ matrix A in the difference equation (3) relates the state at the previous time step $k-1$ to the state at the current step k. The $n \times l$ matrix B relates the optional control input $u \in R^l$ to the state x_k. The $m \times n$ matrix H in the measurement equation (4) relates the state to the measurement z_k.

We define $\hat{x}_k^- \in R^n$ (note the "super minus") to be a prior state estimation at step k given knowledge of the process prior to step k, and $\hat{x}_k \in R^n$ to be a posterior state estimate at step k given measurement z_k. We then define *a priori* and *a posteriori* state estimate errors as

$$e_k^- = x_k - \hat{x}_k^- \tag{7}$$

$$e_k = x_k - \hat{x}_k \tag{8}$$

The *a priori* estimate error covariance is then

$$P_k^- = E[e_k^- e_k^{-T}] \tag{9}$$

And the *a posteriori* estimate error covariance is

$$P_k = E[e_k e_k^T] \tag{10}$$

The Kalman filter estimates a process by using a form of feedback control: the filter estimates the process state at some time and then obtains feedback in the form of (noise) measurement. As such, the equations for the Kalman filter fall into two groups: time update equations and measurement update equations. The time update equations are responsible for projecting forward (in time) the current state and error covariance estimates to obtain *a priori* estimates for the next time step. The measurement update equations are responsible for the feedback, i.e. for incorporating a new measurement into the *a priori* estimate to obtain an improved *a posteriori* estimate [13].

The specific equations for the time and measurement updates are presented below.

Discrete Kalman filter time update equations are

$$\hat{x}_k^- = A\hat{x}_{k-1}^- + Bu_{k-1} \tag{11}$$

$$P_k^- = AP_{k-1}A^T + Q \tag{12}$$

Discrete Kalman filter measurement update equations are

$$K_k = P_k^- H^T (HP_k^- H^T + R)^{-1} \tag{13}$$

$$\hat{x}_k = \hat{x}_k^- + K_k(z_k - H\hat{x}_k^-) \tag{14}$$

$$P_k = (I - K_k H)P_k^- \tag{15}$$

After each time and measurement update pair, the process is repeated with the previous *a posteriori* estimates used to project or practical implementations much more feasible than (for example) an implementation of a Wiener filter [14] which is designed to operate on all of the data directly for each estimate.

3.4. Noise estimation based on Kalman filtering

Step 1: Monte Carlo procedure for noise estimation of ideal good circuit

Due to the tolerance of analog components, the fault-free output voltage is not exactly equal to the response derived from the transfer function of the CUT. So, in order to get the

actual response of the CUT, it is indispensable to apply the Monte Carlo simulation to estimation of the mean and variance of the output signal, respectively.

Step 2: The Kalman filter procedure for noise estimation of an actual good circuit

Owing to the environmental noise impact, the current distribution is not equal to the density distribution calculated in Step 1. Thus, it is reasonable to use the ideal fault-free response as x_{k-1} in eq.(1) and the output coming from the actual circuit as y_k of eq.(2). Using the Kalman filter method, we adjust the variance of w_{k-1} to make the Euclidean distance between the ideal fault-free response and actual fault-free response minimal, at that moment, the variance of w_{k-1} is supposed to be the variance of the distribution of the actual fault-free response.

Step 3: The Kalman filter procedure for noise estimation of a faulty circuit

Because each fault corresponds to one concrete Gaussian distribution, the fault can be located if the distribution is identified. The concrete implementation is as follows.

a) The mean and variance are set to zero and a small positive real number σ_0, respectively. Then one specific Gaussian is obtained.
b) Using the Kalman filter to estimate the current state x_k, where x_{k-1} is the actual fault-free output in eq.(1), and the faulty output is viewed as the measured signal of current state y_k in eq.(2).
c) Calculate the Euclidean distance between x_k and the measured faulty output y_k. If the Euclidean distance meets the certain minimum requirement, stop the process and the corresponding variance in eq.(1) is what we want. Else increase σ_i to σ_{i+1} and set σ_{i+1} as the new variance of Gaussian distribution, and then go to step b).

The Euclidean distance is defined as

$$d(x,y)=\left[\sum_{j=1}^{n}(\xi_j-\eta_j)^2\right]^{1/2} \tag{16}$$

where $x=(\xi_1,\xi_{2,},...,\xi_n), y=(\eta_{1,}\eta_{2,},...,\eta_n)$ represent data sequence.

3.5. Entropy analysis for signature extraction

Thanks to the Kalman filter based method in Section 3.4, the distribution corresponding to a concrete fault is obtained. Then we use Shannon's entropy to get the fault signature

Given $p_i(i=1,...,n)$ represents the probability of event i happening, Shannon's entropy is defined:

$$H(p_1,p_2\ldots,p_n)=\sum_{i=1}^{n}p_i\log_2\frac{1}{p_i} \tag{17}$$

Here, we use the base 2 for the logarithm function in Shannon's entropy. The continuous version of Shannon's entropy is

$$H(p)=\int_{-\infty}^{+\infty}p(x)\log_2\frac{1}{p(x)}dx \tag{18}$$

where $p(x)$ denotes the probability distribution of the system. Here, based on our assumption, $p(x)$ is the Gaussian distribution, that is, $p(x)$ has the form:

$$p(x) = \frac{1}{\sqrt{2\pi}\sigma} \exp(-\frac{x^2}{2\sigma^2}) \tag{19}$$

where σ represents the variance of Gaussian distribution

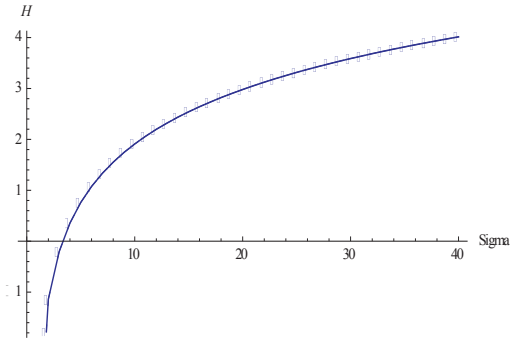

Fig. 2. Signature extraction using Shannon's entropy. X-axis denotes the variance of Gaussian distribution, Y-axis denotes Shannon's entropy

From Fig.2, it is easily seen that the Shannon entropy is a monotone function related to the variance of Gaussian distribution. So Shannon's entropy is unique for a definite Gaussian distribution with a fixed variance.

Therefore, Shannon's entropy could be used as a tool for signature compression, that is to say, if the variance of Gaussian distribution is different, the Shannon entropy is also different. Because different faults result in different variance of Gaussian distribution, the Shannon entropy can be used as the unique signature for a concrete fault of CUT.

In fact, the physical explanation of Shannon's entropy is the information used to be captured from imprecise knowledge that the noise contains. The higher the Shannon entropy, the worse the system quality is.

3.6. Classifier

We use the minimum variance principle as the criteria to match the fault(s), that is, we calculate the Euclidean distance between the predefined fault signature and the one obtained from the proposed method based on the measured output of the CUT. Once the minimum is found, the corresponding fault is regarded as the fault which had happened in the actual analog circuit.

3.7. Algorithm of the signature extraction of the proposed diagnosis scheme

To make the above description of the noise estimation and signature extraction more clear, the flow diagram is used to help arrive at our purpose, that is, Fig.3 and Fig.4, which are employed to exhibit the process of producing the fault-free signature and the faulty signature of the analog circuit under test (CUT) via Kalman filtering and Shannon's entropy techniques, respectively.

It is noted that the generation of the signature of the fault-free analog circuit needs Monte Carlo simulation before using the Kalman filtering technique, that is because for actual testing scenario, the actual fault-free noise and its signature are also needed to estimate effectively when there is no effective reference response for calculation.

It is also worth noting that the initial value of the variance σ_i (or σ_j) can be a rather big number, and decrease with a fixed step until the norm requirement is satisfied, in fact, the initial value of the variance can also be set to be a small number and increase with a fixed step until the corresponding norm condition is fulfilled. In our practice, we set the initial value of σ_i (or σ_j) as 0.01 deviated from its nominal value of variance and the increased scheme is employed to execute the iterative process.

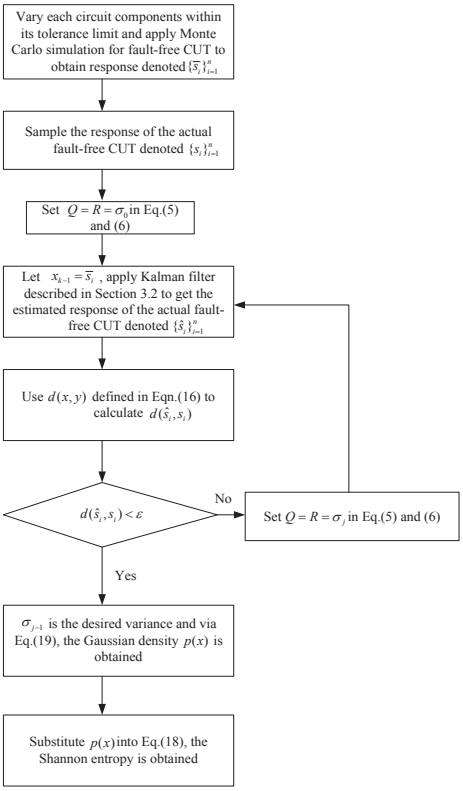

Fig. 3. Algorithm for fault-free signature extraction.

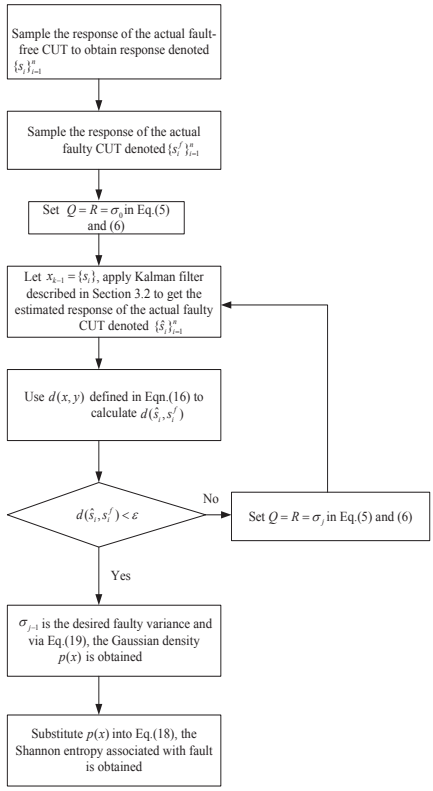

Fig. 4. Algorithm for fault signature extraction.

4. Simulations

Here, simulations will be carried out to illustrate the idea of this paper. All simulation work is finished in a personal computer with a 3-GHz processor and 1-GB random access memory. The programs used in the simulations are developed by the authors in MATLAB.

4.1. Simulation 1- Leapfrog filter circuit

Results of applying the proposed method to a benchmark circuit are explained in this section. The leapfrog filter circuit in Fig.5 is from [18]. All the resistors are $10\,k\Omega$, and capacitor C_1 and C_4 are 0.01 μF, and capacitors C_2 and C_3 are 0.02 μF. The leapfrog filter is a kind of low pass filter, which is based on MITEL semiconductor's complementary metal-oxide-semiconductor (CMOS) technology.

Several faults are inserted into the leapfrog filter, and the filter is simulated with a sinusoidal input of 1 kHz frequency and $\pm 1.5V$ amplitude. The simulation is done using PSPICE. The sampling frequency is 200 kHz and a total of 2048 samples were gathered in 10ms. The simulation results are given in Table I. In the table, "% error" means the error between a faulty circuit and the fault-free circuit in percentage and is the biggest by calculation. $\hat{\sigma}$ denotes estimated variance of the Gaussian distribution.

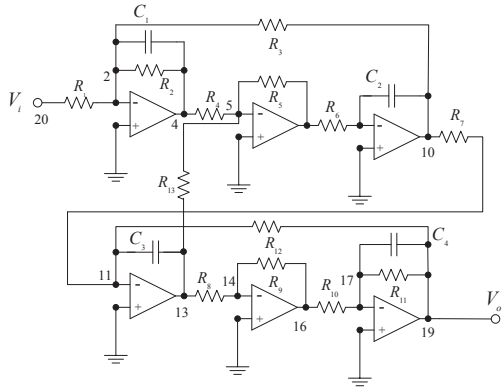

Fig. 5. Leapfrog filter.

TABLE I
RESULTS OF SIGNATURE ANALYSIS USING KALMAN FILTER METHOD FOR FAULT LOCATION IN THE LEAPFROG FILTER

Fault No.	Fault	Faulty value	$\hat{\sigma}$ value	(%error)	Shannon entropy value H
1	Node 10&4 short	100Ω	1.0018+0.02	(2.0)	2.078
2	Node 20&4 short	100Ω	1.0018+1.20	(119.8)	3.186
3	Node 20&10 short	100Ω	1.0018+0.60	(59.9)	2.727
4	Node 5&2 short	100Ω	1.0018+0.80	(79.9)	2.897
5	Node 19&10 short	100Ω	1.0018+0.04	(3.0)	2.106
6	Node 16&13 short	100Ω	1.0018+0.01	(1.0)	2.064
7	Node 16&17 short	100Ω	1.0018+0.70	(72.2)	2.814
8	Node 19&13 short	100Ω	1.0018+0.03	(3.1)	2.092
9	R2 open	1$M\Omega$	1.0018+0.45	(46.4)	2.585
10	R3 open	1$M\Omega$	1.0018+0.29	(29.9)	2.415
11	R5 open	1$M\Omega$	1.0018+0.15	(15.5)	2.251
12	R9 open	1$M\Omega$	1.0018+0.35	(36.1)	2.482
13	R10 open	1$M\Omega$	1.0018+0.41	(42.3)	2.545
14	R2 variation (10k->8k)	8$k\Omega$	1.0018+0.05	(5.1)	2.120
15	R3 variation (10k->8k)	8$k\Omega$	1.0018+0.07	(7.1)	2.147
16	R7 variation (10k->7.5k)	7.5$k\Omega$	1.0018+0.18	(18.3)	2.288
17	R12 variation (10k->8k)	8$k\Omega$	1.0018+0.16	(16.2)	2.263
18	C3 variation (0.02u->0.03u)	0.03u	1.0018+0.47	(47.7)	2.605
0	Actual fault-free	*	1.0018	(0)	2.050

For a catastrophic fault, the proposed method gives good results for fault location. Because of the length limitation and the emphasis of this paper, only the randomly selected four catastrophic faults are analyzed.

In Table I, for example, for cases 1-4, all the values of Shannon's entropy are different from the fault-free case, clearly a 100% detectable rate.

It is also noted that the Shannon entropy in case 1, case 2, case 3, case 4 are 2.078, 3.186, 2.727, 2.897, respectively, and 2.050 for fault-free circuit, which is unique for different faults. So the different fault cases can be separated easily using Shannon's entropy as the signature.

The parametric faults are more complicated since variations of faulty elements are smaller than those of the catastrophic faults. The proposed method can also give good results for locating the parametric fault. For example, the Shannon entropy for case 14 in Table I is 2.120, whereas the value of case 15 is 2.147. The signatures for case 14 and case 15 are different, so these two faults can be separated definitely. The same conclusion can also be drawn for other fault cases in Table I.

TABLE II
ROBUSTNESS COMPARISON BETWEEN COHERENCE FUNCTION RESULTS AND SHANNON'S ENTROPY RESULTS FOR FAULTS 14 AND 15 IN TABLE 1

Data Bank No.	Fault	Coherence Function (subband No.)	Shannon's entropy value *H*
1	R2 variation (10k->8k)	3.21(5)	2.1197
2	R2 variation (10k->8k)	-1.82(5)	2.1201
3	R2 variation (10k->8k)	1.57(5)	2.1197
4	R2 variation (10k->8k)	3.23(5)	2.1198
5	R2 variation (10k->8k)	1.97(5)	2.1202
6	R2 variation (10k->8k)	1.68(5)	2.1211
1	R3 variation (10k->8k)	-0.011(7)	2.1469
2	R3 variation (10k->8k)	-0.005(7)	2.1467
3	R3 variation (10k->8k)	-0.015(7)	2.1473
4	R3 variation (10k->8k)	-0.009(7)	2.1473
5	R3 variation (10k->8k)	-0.014(7)	2.1474
6	R3 variation (10k->8k)	-0.018(7)	2.1474

Because a robust fault signature can dramatically reduce the probability of aliasing, here an analysis will be given to illustrate the robustness of the signature produced by the proposed approach. The method presented in [10] is employed for comparison. The parametric faults for analysis are fault cases 14 and 15 in Table I. The results of comparison are shown in Table II.

From Table II, we see that the method proposed in [10] gives good discrimination for different parametric faults, but its signature, that is, the value of coherence function is not robust. For example, the maximal value of the coherence function of case 14 is 3.21, and the minimal value is 1.57 (for a negative value, we take its absolute value). The biggest relative error is 104.5% for the signature used in the method [10]. Whereas the biggest relative error is only 0.06% when the Shannon entropy is used as the signature based on the Kalman filter method. For fault case 15, the same conclusion can also easily be drawn from Table II.

Since signature with the property of big variation is prone to aliasing, which makes the fault location impossible eventually, a robust signature could greatly reduce the aliasing probability and make the fault detection and location more easily. Thus, the signature produced by using the proposed method is much more efficient than that of using the method in [10] for fault diagnosis of analog circuits.

Fig.6 shows the original fault response and the fault-free output. The fault response estimated by using the proposed method is depicted in Fig.7

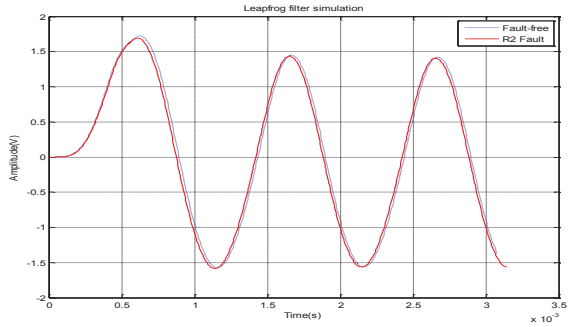

Fig. 6. Leapfrog filter: Fault-free response (blue dotted line) and R2 parameter fault response (red solid line). X-axis denotes the time (s), Y-axis denotes the amplitude (v).

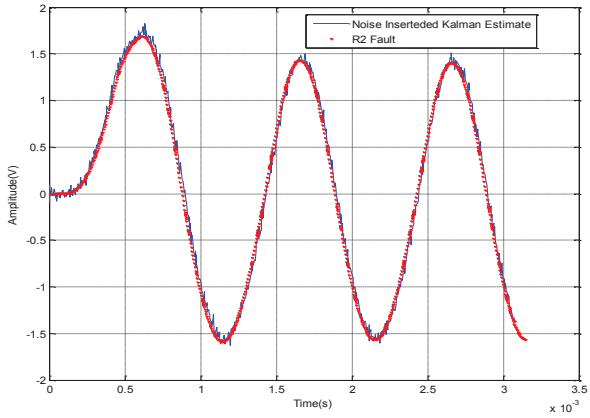

Fig. 7. Leapfrog Filter: The Kalman filter based method for realization of the R2 parametric fault response (red dotted line) by using the fault-free response plus Gaussian white noise with a proper variance (blue solid line). X-axis denotes the time (s), Y-axis denotes the amplitude (v).

4.2. Simulation 2 - State variable filter circuit

The state variable filter [18] in Fig.8 is used as the second benchmark circuit for the simulation. All the capacitors are 0.02 μF and all the resistors are 10 $k\Omega$ except R_2, R_2 =3 $k\Omega$. The input to system is a 1- kHz sinusoidal signal and the output of the system is measured at the band pass output pin. The sampling frequency is 25 kHz and samples are gathered for 10.24ms.

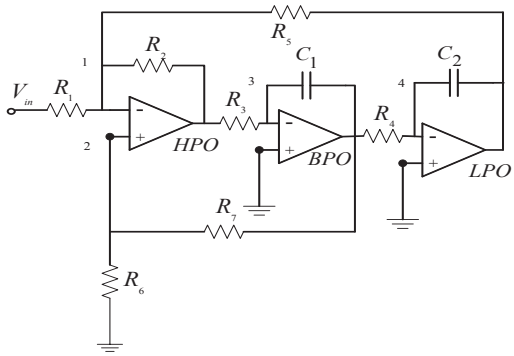

Fig. 8. State variable filter.

Fifteen fault cases including six catastrophic faults and nine parametric faults are considered. All of the fault cases are randomly given. The testing results are shown in Table III, where "% error" means the error between a faulty circuit and the fault-free circuit in percentage and is the biggest by calculation. $\hat{\sigma}$ denotes the estimated variance of Gaussian distribution.

From Table III it is easily seen that the proposed method can locate catastrophic faults effectively, as is the parametric faults. That is, there is a one-to-one mapping between the fault and the Shannon entropy, which is used for signature in our scheme. For example, the Shannon entropy of fault case 1 is 1.81 and that of case 3 is 1.95, they are all different from the Shannon entropy of the fault-free case, and since they are not equal, these two fault cases can be discriminated easily. The same conclusion can also been drawn for any other fault cases in Table III. Further, because of the robustness of the Shannon entropy, the signature we derived here is nearly a constant, so the declaration of the fault for the CUT is more reliable.

TABLE III
RESULTS OF SIGNATURE ANALYSIS USING KALMAN FILTER METHOD FOR FAULTS LOCATION IN THE STATE VARIABLE FILTER

Fault No.	Fault	Faulty value	$\hat{\sigma}$ value (%error)	Shannon entropy value H
1	Node 1&3 short	100Ω	0.68631+0.16 (23.31)	1.8063
2	Node 3&4 short	100Ω	0.68631+0.02 (2.91)	1.5455
3	Node 1&4 short	100Ω	0.68631+0.25 (36.43)	1.9522
4	Node 1&3 open	1*M*Ω	0.68631+0.015 (2.19)	1.5352
5	Node 1&4 open	1*M*Ω	0.68631+0.011 (1.60)	1.5270
6	Node 4&3 open	1*M*Ω	0.68631+0.009 (1.31)	1.5228
7	R2 variation (3k->2.4k)	2.4*k*Ω	0.68631+0.1 (14.57)	1.7003
8	R3 variation (10k->8k)	8*k*Ω	0.68631+0.14 (20.40)	1.7719
9	R1 variation (10k->7.5k)	7.5*k*Ω	0.68631+0.18 (26.23)	1.8401
10	R4 variation (10k->8k)	8*k*Ω	0.68631+0.036 (5.25)	1.5778
11	R5 variation (10k->8k)	8*k*Ω	0.68631+0.038 (5.54)	1.5812
12	R6 variation (10k->8k)	8*k*Ω	0.68631+0.048 (6.99)	1.6016
13	R7 variation (10k->8k)	8*k*Ω	0.68631+0.005 (0.73)	1.5145
14	C1 variation (0.02u->0.03u)	0.03*u*	0.68631+0.013 (1.89)	1.5311
15	C2 variation (0.02u->0.03u)	0.03*u*	0.68631+0.023 (3.35)	1.5516
0	Actual fault-free	*	0.68631 (0)	1.5040

5. The Experiment

Other than the simulations, an experiment is carried out on the actual circuit to verify the proposed method.

The circuit under test is Tow-Thomas filter circuit. The structure and parameters of this circuit [18] are illustrated in Figure 9, that is, $R_1 = R_2 = R_3 = R_4 = 16k\Omega$, $R_5 = R_6 = 10k\Omega$, $C_1 = C_2 = 1nF$. The actual circuit is shown in Figure 10, and the amplifiers in the circuit are TL084 produced by TI. The circuit is stimulated by a 1V, 10 kHz sinusoidal signal, and the output of the fault-free and faulty circuit are measured by an oscilloscope produced by Tektronix. The sample rate of the oscilloscope is 1GS/s and its band width is 100M. Eight fault cases are randomly chosen, and the test results are listed in Table IV.

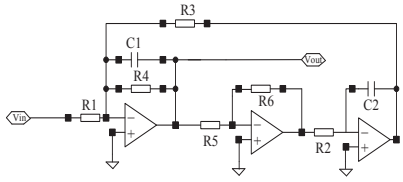

Fig. 9. Tow-Thomas filter.

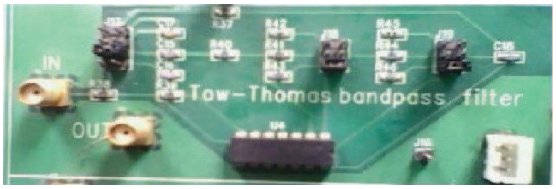

Fig. 10. The actual Tow-Thomas filter.

In Table IV, fault 1 and fault 2 represent two types of parametric faults of one component, that is, for fault 1, the value of component C1 is smaller than its nominal value, whereas for fault 2, the value is bigger than the nominal value of C1. The same is the case with fault 3 and fault 4, fault 5 and fault 6, respectively. Fault 7 is a multiple parametric fault caused by the variations of the C1 and R6 and R2 together. Fault 6 is the same case as fault 7.

Table IV is also an illustration of the good discrimination effects for different parametric faults in an analog circuit by using the proposed method. All the results show that the faults can be precisely located without aliasing. For example, for fault case 1, the Shannon entropy is -0.8253, whereas its value is -0.8466 for fault case 2. They are different values and all of them are not equal to the value of the fault-free circuit, so fault case 1 and fault case 2 can easily be separated. The same conclusion can be drawn for any other cases as well.

TABLE IV
RESULTS OF SIGNATURE ANALYSIS USING KALMAN FILTER METHOD FOR FAULT LOCATION IN THE TOW-THOMAS FILTER

Fault No.	Fault	Faulty value	$\hat{\sigma}$ value	(%error)	Shannon entropy value H
1	C1 Variation (1nF->0.82nF)	$0.82nF$	0.13156+0.0050	(3.80)	-0.8253
2	C1 variation (1nF->1.2nF)	$1.2nF$	0.13156+0.0030	(2.28)	-0.8466
3	R6 variation (10k->9.1k)	$9.1k\Omega$	0.13156+0.0060	(4.56)	-0.8147
4	R6 variation (10k->11k)	$11k\Omega$	0.13156+0.0040	(3.04)	-0.8359
5	R2 variation (16k->14.7k)	$14.7k\Omega$	0.13156+0.0035	(2.66)	-0.8412
6	R2 variation (16k->16.9k)	$16.9k\Omega$	0.13156+0.0067	(5.09)	-0.8074
7	Fault 1 + Fault 3 + Fault 5	$0.82nF + 9.1k + 14.7k$	0.13156+0.0070	(5.32)	-0.8043
8	Fault 2 + Fault 4 + Fault 6	$1.2nF + 11k + 16.9k$	0.13156+0.0005	(0.38)	-0.8736
0	Fault free	*	0.13156 (0)		-0.8791

TABLE V
ROBUSTNESS OF SIGNATURE BY USING KALMAN FILTER BASED METHOD FOR DIAGNOSIS IN THE TOW-THOMAS FILTER

No.	Fault	Faulty value	$\hat{\sigma}$ value	Shannon entropy value H
1	C1 Variation (1nF->0.82nF)	$0.82nF$	0.13156+0.00501	-0.8252
2	C1 Variation (1nF->0.82nF)	$0.82nF$	0.13156+0.00502	-0.8251
3	C1 Variation (1nF->0.82nF)	$0.82nF$	0.13156+0.00501	-0.8252
4	C1 Variation (1nF->0.82nF)	$0.82nF$	0.13156+0.00503	-0.8250
5	C1 Variation (1nF->0.82nF)	$0.82nF$	0.13156+0.00501	-0.8252
6	C1 Variation (1nF->0.82nF)	$0.82nF$	0.13156+0.00502	-0.8251
7	C1 Variation (1nF->0.82nF)	$0.82nF$	0.13156+0.00501	-0.8252
8	C1 Variation (1nF->0.82nF)	$0.82nF$	0.13156+0.00501	-0.8252
9	C1 Variation (1nF->0.82nF)	$0.82nF$	0.13156+0.00501	-0.8252
10	C1 Variation (1nF->0.82nF)	$0.82nF$	0.13156+0.00501	-0.8252
11	C1 Variation (1nF->0.82nF)	$0.82nF$	0.13156+0.00502	-0.8251
12	C1 Variation (1nF->0.82nF)	$0.82nF$	0.13156+0.00501	-0.8252

Furthermore, the multiple parametric faults can also be located by using the proposed method. For example, for fault 7, its signature - the Shannon entropy is -0.8043, while for fault 8, its signature value is -0.8736, which is different from the value of fault case 7, thus these two multiple parametric faults can both be located.

Especially, the signature obtained by using the proposed method also shows strong robustness for an actual circuit. For example, shown in Table V, the fault case 1 in Table IV is considered, that is, the C_1 down drift parametric fault, the difference between its maximal signature value and minimal value is only 0.0001. So, the probability of aliasing is greatly reduced by using the proposed method for the fault diagnosis of actual analog circuits.

6. Conclusions

A signature with robust discrimination capacity is crucial for fault location in analog circuits. The noise-aid scheme provides a way to produce the robust signatures. When faults occur, one special noise corresponding to the faults arises. To use the information contained in the noise for signature extraction, a new fault model and a noise estimation method for fault location in analog circuits have been proposed in this paper. The approach combines Kalman filtering with Shannon's entropy to analyze the signature in analog circuits. Simulations and experimental results show that the approach provides a robust signature both for catastrophic faults and parametric faults. Based on these signatures, the parametric faults and the catastrophic faults in analog circuits can be located effectively and reliably.

Compared with the existing method (the subband method employing coherence function [10]), the approach is this paper can produce a more stable signature in locating parametric components in analog circuits. So the proposed method improves the discrimination capacity strongly. The simulation examples and experimental results show the advantages.

Further, the proposed method only requires the measurement of the output signal from the system primary output pins so that both the parasitics and the testing cost are reduced.

Since the Kalman filter can be built with a small hardware cost, the proposed approach in this paper can be used for the on-line testing scenario. Unfortunately, the proposed method can only be applied to the diagnosis of linear analog circuits due to the limitation introduced by the Kalman filter. However, with the help of nonlinear Kalman filter methods, such as the extended Kalman filter (EKF), the approach in this paper can also be extended to diagnose the fault in nonlinear analog circuits, and this will be our future work. The reader is invited to attack this problem.

Acknowledgements

The authors would like to thank the National Natural Science Foundation of China (Grant no. 60871056 & no. 90407007) and the Specialized Research Fund for the Doctoral Program of High Education of China for their support of this research.

References

[1] Starzyk, J. A., Liu, D., Nelson, D.E., Rutkowski, J.O. (2004). Entropy-based optimum test nodes selection for the analog fault dictionary techniques and implementation. *Transactions on Instrument & Measurement,* 53(3), 754-761.

[2] Duhamal, P, Rault, J.C. (1979). Automatic tests generation techniques for analog circuits and systems: a review. *Transactions on Circuits and Systems, I.,* VAS-26, 440-441.

[3] Bandler, J.W., Salama A.E. (1981). Fault diagnosis of analog circuits. *Proc.IEEE*, 73, 1279–1325.

[4] Roh, J., Abraham, J.A. (2004). Subband filtering for time and frequency analysis of mixed-signal circuit testing. *IEEE Transactions on Instrument & Measurement,* 53(2), 602-611.

[5] Papakostas, D.K., Hatzopoulos, A.A. (1993). Correlation-based comparison of analog signatures for identification and fault diagnosis. *IEEE Transactions on Instrument & Measurement,* 42(4), 860-863.

[6] Catelani, M., Fort, A. (2000). Fault diagnosis of electronic analog circuits using a radial function network classifier. *Measurement,* 28, 147-154.

[7] Guo, Z, Savir, J. (2006). Coefficient-based test of parametric faults in analog circuits. *IEEE Transactions on Instrument & Measurement,* 55(1), 150-157.

[8] Savir, J., Guo, Z. (2002). On the detectability of parametric faults in analog circuits. *IProc.Int.Conf. Computer Design (ICCD)*. Freiburg, Germany, Sep., 273-276.

[9] Yang, C., Tian, S., Long, B., Chen, F. (2011). Methods of handling the tolerance and test-point selection problem for analog-circuit fault diagnosis. *IEEE Transactions on Instrument & Measurement,* 60(1), 176-185.

[10] Deng, Y., Shi, B., Zhang, W. (2012). An approach to locate parametric faults in nonlinear analog circuits. *IEEE Transactions on Instrument & Measurement,* 61(2), 358-367.

[11] Kalman, R.E. (1960). A new approach to linear filtering and prediction problems. *Transaction of the ASME-Journal of Basic Engineering*, 34-45.

[12] Grewal, M.S., Andrew, A.P. (2008). Kalman filtering: Theory and Practice using MATLAB. Third edition, Wiley&Sons Inc., 1-2.

[13] Welch, G., Bishop, G. (2002). An introduction to the Kalman filter. Available:*http://www.cs.unc.edu/Welch/kalman/kalmanIntro.html*.

[14] Brown. R.G., Hwang. P.Y.C. (1992). Introduction to random signals and applied Kalman filtering. Second edition. Wiley&Sons, Inc.

[15] Ando. B., Graziani. S. (2001). Adding noise to improve measurement. *IEEE Trans. Instrum. & Meas.Magazine*. 4(1). 24-31.

[16] Kay, S. (2008). Noise enhanced detection as a spectral case of randomization. *IEEE Signal Process. Lett*. 15. 709-712.

[17] Chen, H., Varshnew, P.K., Kay, S., Michels, J.H. (2009). Noise enhanced nonparametric detection. *IEEE Trans. Inf. Theory,* 55(2), 499-506.

[18] Kaminska, B., Arabi, K., Bell, I., Huertas, J.L., Kim, B., Rueda, A., Soma, M. (1997). Analog and mixed-signal benchmark circuits-first release. *Proc. IEEE Int. Test Conf. [Online]*,183-190.